Unmanned Systems, Vol. 10, No. 1 (2022) 31–43

DOI: 10.1142/S2301385022500017

UNMANNED SYSTEMS
https://www.worldscientific.com/worldscinet/us

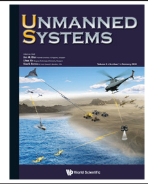

A Novel Mini Jet Engine Powered Unmanned Aerial Vehicle: Modeling and Control*

Erdinç Altuğ[†], Abdullah Türkmen

Autonomous Systems Research Laboratory,
Department of Mechanical Engineering,
Istanbul Technical University,
İnönü Caddesi No: 65, Beyoğlu,
Istanbul 34437, Turkey

Significant progress has been made in recent years on personal air vehicles (PAVs), which offer independent and autonomous urban transportation. On-demand parcel delivery drones and heavy-lift drones are gaining serious attention. Although various designs for these systems have been put forward, they still have not reached sufficient maturity. The current systems provide somehow satisfactory operation, but many of these systems are limited in payload capacity and flight duration, and not suitable for future operations. In this paper, we propose a novel thrust system that uses multiple mini jet engines. Unlike electric motors, the jet engine thrust cannot vary rapidly. This led us to design and develop a thrust vectoring system for each jet engine. This proposed system has the potential to enable drones to carry more payload and achieve longer flight times. This paper discusses the design and modeling of the system as well as the stabilization algorithms that satisfactorily stabilize the proposed system. We presented that due to motor lag, thrust variations cannot stabilize the vehicle. We showed that the use of a thrust vectoring mechanism with LQR-based controller can overcome the effects of motor lag and stabilize the vehicle, successfully.

Keywords: UAV; jet engine; thrust vectoring; LQR; flight stability.

US

1. Introduction

Since the beginning of the 21st century, we are witnessing various useful applications of unmanned aerial vehicles (UAVs) [1–8]. These range from taking fascinating drone photos/videos, transport of goods, search and rescue operations to the inspection. These tasks can be performed more economically and rapidly, with almost no risk of human life. These vehicles are more economical, smaller, require smaller landing pads/airstrips, consume less fuel and pollute less, in comparison to manned aircrafts. Moreover, we have seen that these vehicles could also be useful in many previously unsought areas (such as dropping a life vest to a drowning person or ambulance drones). It is expected that as the autonomy level of these systems increases in the decades to follow, they are expected to have greater positive contributions to our lives.

The most common UAV systems are small multi-rotor, electrical systems. Although they are widely used in many operations, their potential usage is limited due to the limits of electrical motors. Electric motors are easy to use and have a short response time, which is the main reason for their ability to fly, but they are also the main reason limiting their potential. The payload capacity, flight time and range are the most critical properties of unmanned aerial vehicles. Although current systems provide somehow suitable operation envelopes, these systems are limited and not suitable for future operations such as parcel delivery and flying taxi operations. Current prototypes of the parcel and taxi drones commonly are scaled-up versions of smaller drones, having the same limitations of flight time and payload capacity, requiring long charging time or battery swaps, which limits their usefulness.

Received 30 September 2020; Revised 11 March 2021; Accepted 11 March 2021; Published 14 May 2021. This paper was recommended for publication in its revised form by editorial board member, Kimon P. Valavanis.
Email Address: †*altuger@itu.edu.tr*
*This paper is an expanded version of our ICUAS 2020 paper.

One alternative to an electrical motor/rotor thrust system is a jet engine. Since the 1960s, they are widely used in various aerial vehicles [9, 10]. Mini jet engines are smaller versions of bigger jet engines and some model aircraft users use them for years. Various companies are working on the design and manufacturing of these mini jet engines [11–15].

There are some studies on the modeling of mini jet engines as well as the design and manufacture of the electronic control unit [16, 17]. In these studies, aerothermodynamic modeling of mini jet engines and verification of the prepared model and control tests were carried out.

There are a few pilot-operated, manually controlled personal jet engine aircrafts with vertical landing and take-off feature. Successful flights were realized with these vehicles [18].

In the literature, there is no autonomous aircraft with vertical landing and take-off capability using mini jet engines. Probably this is due to two reasons. Until recently, it used to be quite difficult to manufacture reliable mini jet engines. Another reason is the difficulty in thrust control of jet engines compared to electric motors. The dynamic behavior of jet engines is slower than electric engines and it does not allow to control the VTOL aircraft just like it is done in electric motor/rotor pairs.

In the literature, some aircrafts use ducted fans that work with electric motors and batteries [19, 20]. Although they may look similar to jet engines, they are different. In [21], ducted fan impulse sources are used. There is an aircraft developed in the light of this patent [22].

Some aircrafts in the literature use electric motors and are able to tilt rotors to vector thrust [23–30]. These vehicles have more control over the aircraft than normal four-rotor aircraft. Similarly, Quad Tilt Rotor (QTR) aircraft combines VTOL quadrotor with aircraft form [27, 28, 31].

In our previous study, we proposed a multi-rotor vehicle that can rotate all four rotors in two axes [32–35]. Such a design can provide a more stable flight without the need for the vehicle body to bend in the direction of motion.

In recent years, proposed prototypes on flying taxis and cars for human transportation have become prominent [36]. These studies also require a more reliable thrust solution.

In this paper, modeling and control of a jet-powered mini VTOL vehicle (quad-jet) is proposed. The introduction of increased payload capacity, as well as VTOL ability and autonomous operation, can greatly improve civilian applications. The ability to direct the thrust on each engine with the help of a novel two-degree-of-freedom tilt mechanism will eliminate the need to change the thrust rapidly. Moreover, the ability to direct the engine thrusts eliminates the need to tilt the robot towards the direction of motion (as multi-rotor aircrafts do), leading to a more stable motion.

In the literature, many different controllers are introduced for UAVs. Although many of these control methods are linear controllers, it is noteworthy that nonlinear controller structures are also used [37, 38]. Model Predictive Control (MPC) and Linear–quadratic regulator (LQR) control strategies have been popular in recent years as a control method in UAVs [20, 39, 40, 41, 42]. Unlike conventional linear and nonlinear control methods, MPC and LQR proved to be quite useful. In this study, we will investigate different controllers such as PID and LQR to stabilize a quad-jet aircraft model. Mathematical models and control structures are simulated in MATLAB Simulink environment.

The paper is organized as follows: Section 2 describes the UAV Platform Design. The modeling of the system is presented in Sec. 3. Section 4 contains the control approach and simulations. Concluding remarks and future work are presented in Sec. 5.

2. UAV Platform Design

A UAV system's propulsion consists of thrust generator and fuel. For an electrical multi-rotor vehicle, this corresponds to electric motors, gears, rotors, and batteries. For a jet-engined system, this corresponds to jet motors and fuel. The comparison of electrical and jet actuation is given in Table 1. Unlike batteries, combustible fuel weight decreases with consumption.

The conventional electrical multi-rotor systems are very simple, cheap, and easy to fly when they are smaller. Unfortunately, they do not scale up efficiently. Although it is quite possible to develop and fly big multi-rotor UAVs that can carry big payloads (e.g. flying taxi operations), this requires heavy, expensive motor and heavy batteries. Moreover, the rotor size needs to be much bigger to obtain the required thrust, leading to a much bigger vehicle size. Additionally, limited useful flight time is generally followed by a long charging time or a battery swap.

For the mini jet engines, the fuel amount can be increased as needed easily. Fuel amount is the limiting factor of flight duration.

The major goal of the system is to extend the payload capacity, flight duration, and range of operation. Unlike an electrical propulsion system consisting of electric motors, rotors, electronic speed controller, and battery, the propulsion system of the proposed vehicle consists of jet engines, a thrust vectoring system, a rigid body, and fuel tanks.

In this section, we will describe the jet engine, the mechanical design of the thrust vectoring system, and the design of the UAV body.

2.1. *The jet engine*

There are various mini jet engines available for the RC community. Some of these engines weigh less than 2 kg and

January 5, 2022 1:19:25pm WSPC/284-US 2250001 ISSN: 2301-3850 2nd Reading

Table 1. Comparison of electrical versus mini jet actuation for heavy-lift UAVs.

Electrical actuation systems	Mini jet engine system
Smaller thrust-to-weight ratio	Bigger thrust-to-weight ratio
Bigger size due to big rotor	Smaller size
Noise level of about 80 dB	Noise level of about 110 dB
Do not require thrust vectoring	Require thrust vectoring
Limited by battery	Limited by fuel weight
Need battery charging	Can be easily refueled rapidly
Suitable for indoors	Not suitable for indoors

provide a lift of 20 kg. The thrust-to-weight ratio is much bigger than the conventional electric motors. In this study, we searched for a jet engine that is reliable, available, affordable, having acceptable fuel consumption characteristics, and with a maximum thrust of about 150 N per engine. The use of four mini jet engines can easily lift a 60-kg vehicle successfully. Unfortunately, the fuel consumption of these jet engines at the full RPM can go up to 10 g/s. Therefore, fuel consumption and flight duration should be investigated before engine selection.

The jet engine in this study has been selected as Jetcat P160 (Fig. 1) [11]. The thrust-to-weight ratio is 9.64 and the fuel consumption is about 7 g/s at the maximum RPM. Technical specifications are given in Table 2.

A test setup has been set up to verify the provided specifications, and to collect engine thrust, motor rpm, fuel level, pump battery ECU battery level, and outlet heat values with respect to throttle value (Fig. 2).

A graphical user interface has been developed to visualize and collect the data automatically (Fig. 3).

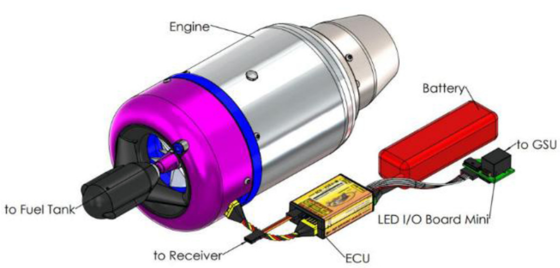

Fig. 1. Jetcat P160 mini jet engine and its parts.

Table 2. Technical specifications of the jet engine.

Name	Value
Weight (g)	1670
Length (mm)	297
Idle thrust (N)	7
Thrust at maximum rpm (N)	158
Specific fuel consumption (SFC) (kg/N·h)	0.160

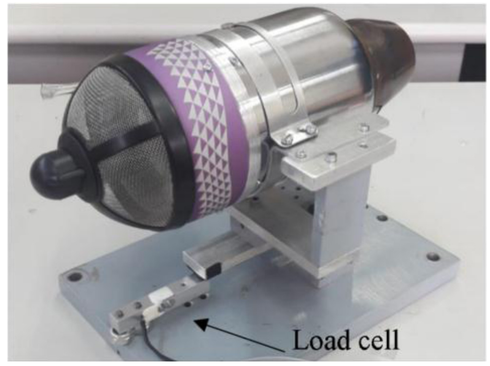

Fig. 2. Mini jet engine test setup.

Thrust experiment on jet engine verified that a thrust of 180 N is possible. The thrust versus time data is shown in Fig. 4.

2.2. *Flight time and payload relationship*

The SFC for the P160 jet engine is 0.16 kg/h per unit thrust. This corresponds to about 5.61 g/s of fuel consumption per jet engine. Total fuel usage is about 1.3 kg/min at 80% thrust. As the fuel is spent, less fuel per minute will be needed to keep the vehicle flying.

The goal of the proposed system is to maximize payload as well as flight time. The fuel takes away useful payload, but its weight decreases with consumption. An algorithm on MATLAB has been developed to clarify the flight and payload relationship. Assuming the maximum total mass of 60 kg and vehicle body mass of 25 kg, this analysis shows the flight time (in min) versus load (kg) in Fig. 5.

It appears that with no load, the vehicle is expected to fly for 101 min. It can lift as much as 35 kg, with a few minutes of flight. If the payload is 18 kg, the flight time is approximately 48 min, which is within the design goals. A more recent model P220 from the same company can provide 220 N with the same SFC value. This engine can lift a vehicle mass up to of up to 80 kg, that can fly as long as 160 min or can lift about 55-kg payload, from the same analysis.

Note that hovering a vehicle with electric or jet-fueled motors is a fuel-consuming task. Well-designed vehicles limit the hover time and use wings for lift, this approach increased flight time by reducing the fuel wasted for hover. The proposed vehicle does not have wings, because it has been designed for lifting and carry a payload within a limited area. It does not have a goal of carrying this payload to a distant location.

2.3. *Design of the thrust vectoring system*

The goal of the thrust vectoring system is to direct the thrust as needed. The thrust vectoring system rotates the

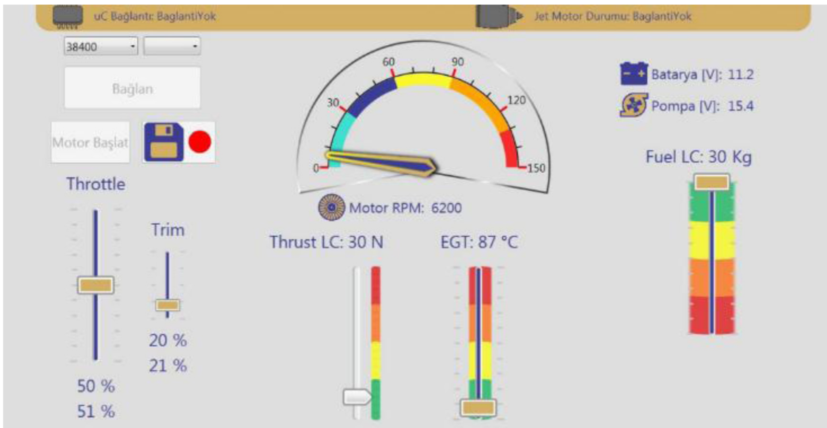

Fig. 3. Graphical user interface for data collection.

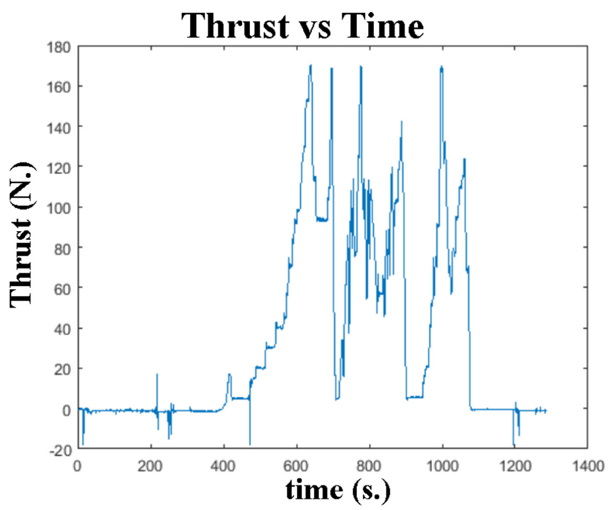

Fig. 4. Thrust versus time plot obtained with experiment.

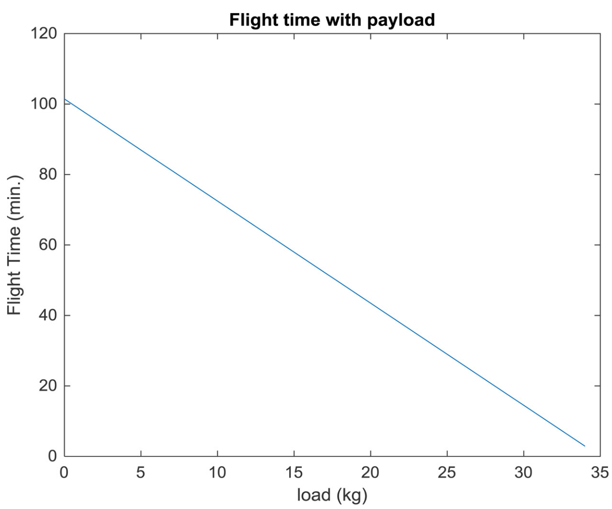

Fig. 5. The flight time versus payload graph for the proposed vehicle.

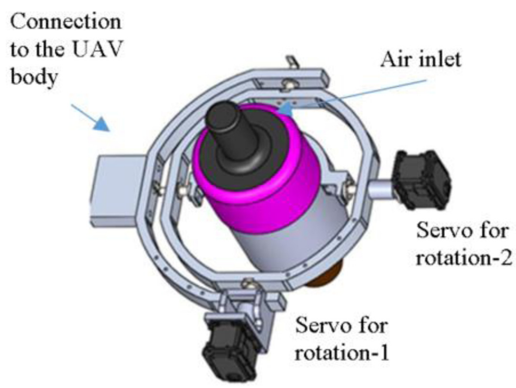

Fig. 6. The thrust vectoring system for controlling thrust forces acting on the UAV.

engine around two axes, independently. Mechanical design considering the structural loads was performed and the design shown in Fig. 6 has been developed.

2.4. *Mechanical design of the UAV*

The aircraft has been designed in CAD under the strict considerations of structural integrity, static loading, as well as weight limits. Figures 7 and 8 show the 3D CAD model of the jet-powered VTOL aircraft, including the engines, the thrust vectoring mechanism, and fuel tanks.

3. Modeling of the Quad-jet System

In this study, the required lift force is provided to the aircraft with four mini jet engines. Considering the slow response times of jet engines compared to electric motors, it is not possible to fly this aircraft only by controlling the thrust of jet engines, like a multi-rotor UAV. To solve this problem, extra degrees of freedom have been added to the

January 5, 2022 1:19:47pm WSPC/284-US 2250001 ISSN: 2301-3850 2nd Reading

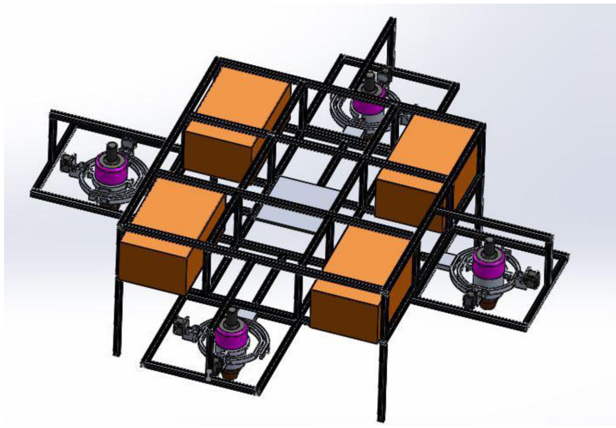

Fig. 7. The 3D design of the UAV platform.

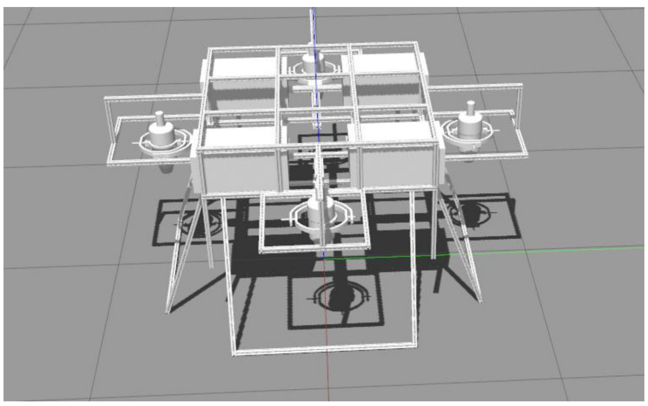

Fig. 8. The 3D model in the simulation environment.

system. While keeping the thrust of each jet engine constant, the direction is rotated along the pitch and roll axes. In this way, two degrees of freedom for each motor (a total of eight degrees of freedom) are added to the system.

In electric motors, a torsion moment (opposite moment occurring in the axis of rotation of the shaft) occurs in the opposite direction of the propeller rotation. In jet engines, on the other hand, due to the structure of the engine, the torsion moment is very low and it is accepted as zero. This eliminates the need for motor pairs to rotate in opposite directions.

Gyroscopic moments that are often neglected in multi-rotor aircraft are more prominent in jet aircraft. Besides, the pitching and rolling movements of each jet engine in its axis cause gyroscopic moments in the body of the aircraft.

3.1. *Coordinate systems*

The free-body diagram of the quad-jet model is displayed in Fig. 9. The aircraft has six different coordinates. The first is

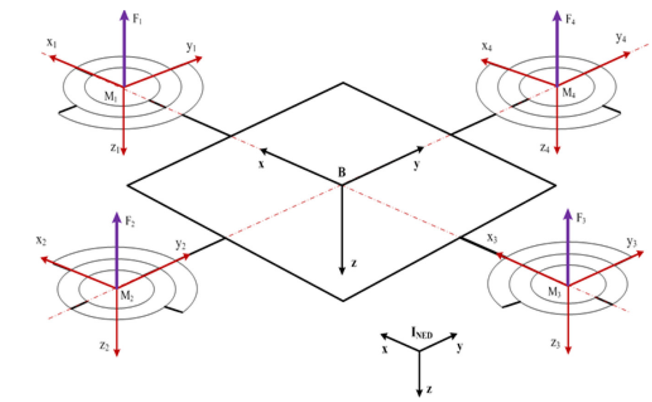

Fig. 9. Jet engine-powered quad-jet UAV free-body diagram, showing the axes.

the inertial reference system, whose unit vectors are oriented to northeast-down and named as I_{NED}. It is positioned on the lower side of Fig. 9. The second reference system is located at the center of mass of the vehicle, labeled as B. This reference system allows the forces and moments created by the engines to be easily formulated. The other four reference systems are also moving reference systems. They are placed in positions where the center of mass of the jet engines are located. These vectors are aligned with the vectors of the B-axis.

3.2. *Euler angles*

Euler angles are widely used to mathematically express the angular orientation of the moving reference systems used in the aircraft. In this study, the ZYX Euler angles representation was preferred. The symbol ψ is used for rotation around the Z-axis, θ for rotation around the Y-axis, and ϕ for the rotation around the X-axis. The rotation matrix, defining the orientation between body axis and inertial reference system, is given as

$$
\begin{aligned}
R &= R_z \cdot R_y \cdot R_x \\
&= \begin{bmatrix} c(\theta)c(\psi) & s(\phi)s(\theta)c(\psi) - c(\phi)s(\psi) & c(\phi)s(\theta)c(\psi) + s(\phi)s(\psi) \\ c(\theta)s(\psi) & s(\phi)s(\theta)s(\psi) + c(\phi)c(\psi) & c(\phi)s(\theta)s(\psi) - s(\phi)c(\psi) \\ -s(\theta) & s(\phi)c(\theta) & c(\phi)c(\theta) \end{bmatrix},
\end{aligned}
$$

where $s(\cdot)$ and $c(\cdot)$ stands for $\sin(\cdot)$ and $\cos(\cdot)$, respectively.

3.3. *Aircraft kinematic and dynamic models*

In this subsection, six-degree-of-freedom equations of motion of the aircraft will be derived. Let us define linear positions as $\{x\ y\ z\}^T$ and angular positions as $\{\phi\ \theta\ \psi\}^T$ with respect to the inertial reference system. Linear and angular velocities of the vehicle are defined as $\{u\ v\ w\}^T$ and $\{p\ q\ r\}^T$ with respect to the B-centered reference system located in the center of mass of the vehicle. The relationship of linear and angular velocities between the B reference system on the vehicle and the inertial reference system is obtained by the following equations:

$$\begin{Bmatrix} \dot{x} \\ \dot{y} \\ \dot{z} \end{Bmatrix} = R_{zyx} \begin{Bmatrix} u \\ v \\ w \end{Bmatrix}, \tag{1}$$

$$\begin{Bmatrix} \dot{\phi} \\ \dot{\theta} \\ \dot{\psi} \end{Bmatrix} = \begin{bmatrix} 1 & \sin(\phi)\tan(\theta) & \cos(\phi)\tan(\theta) \\ 0 & \cos(\phi) & -\sin(\phi) \\ 0 & \dfrac{\sin(\phi)}{\cos(\theta)} & \dfrac{\cos(\phi)}{\cos(\theta)} \end{bmatrix} \begin{Bmatrix} p \\ q \\ r \end{Bmatrix}, \tag{2}$$

There are different sources of force and moment that affect the aircraft, mainly jet engines, gravity, and wind. These forces and moments are used when obtaining the dynamic equations of the vehicle. Considering Newton's law of motion and the Euler equations, the relationship between forces and moments affecting the aircraft and the motion of the vehicle is obtained with the following equations.

$$\begin{Bmatrix} F_{B_x} \\ F_{B_y} \\ F_{B_z} \end{Bmatrix} = m\left(\begin{Bmatrix} p \\ q \\ r \end{Bmatrix} \times \begin{Bmatrix} u \\ v \\ w \end{Bmatrix} + \begin{Bmatrix} \dot{u} \\ \dot{v} \\ \dot{w} \end{Bmatrix}\right), \tag{3}$$

$$\begin{Bmatrix} M_{B_x} \\ M_{B_y} \\ M_{B_z} \end{Bmatrix} = \begin{bmatrix} I_x & 0 & 0 \\ 0 & I_y & 0 \\ 0 & 0 & I_z \end{bmatrix} \cdot \begin{Bmatrix} \dot{p} \\ \dot{q} \\ \dot{r} \end{Bmatrix} + \begin{Bmatrix} p \\ q \\ r \end{Bmatrix} \cdot \left(\begin{bmatrix} I_x & 0 & 0 \\ 0 & I_y & 0 \\ 0 & 0 & I_z \end{bmatrix} \cdot \begin{Bmatrix} p \\ q \\ r \end{Bmatrix}\right), \tag{4}$$

where F_B and M_B represent forces and moments acting on the vehicle and represented in B reference frame. The aircraft is assumed to be symmetric with respect to the B reference frame, resulting in a diagonal inertia matrix,

$$\begin{Bmatrix} F_{B_x} \\ F_{B_y} \\ F_{B_z} \end{Bmatrix} = \begin{Bmatrix} F_{m_x} \\ F_{m_y} \\ F_{m_z} \end{Bmatrix} + \begin{Bmatrix} F_{g_x} \\ F_{g_y} \\ F_{g_z} \end{Bmatrix} + \begin{Bmatrix} F_{d_x} \\ F_{d_y} \\ F_{d_z} \end{Bmatrix}. \tag{5}$$

The total force acting on the vehicle (F_B) is due to jet engines (F_m), gravity (F_g), and drag (F_d). The aircraft is planned to hover or perform slow flights. For this reason, drag forces were ignored in this model.

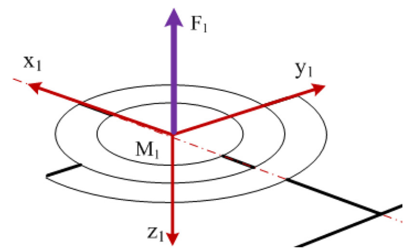

Fig. 10. Coordinate axis for a single jet engine.

Each motor can be rotated around y- and x-axes as shown in Fig. 10, resulting in a change in the direction of the thrust of the engine. The rotation in each motor is represented by Euler angles θ_i and ϕ_i, i.e. $i = 1, 2, 3, 4$. Here again the ZYX convention is used, and the rotation around Z is taken as zero.

The thrust force in the engine is directed upward when θ_i and ϕ_i angles of the thrust vectoring mechanisms are zero, causing a force vector $\{0\ 0\ -F_i\}^T$ in the body-fixed frame. When this force vector is multiplied with the rotation matrix, the thrust force vector expressed in the body fixed frame is obtained as follows:

$$\begin{Bmatrix} F_{m_x} \\ F_{m_y} \\ F_{m_z} \end{Bmatrix}_i = \begin{Bmatrix} -F_i \sin\theta_i \cos\phi_i \\ F_i \sin\phi_i \\ -F_i \cos\theta_i \cos\phi_i \end{Bmatrix}. \tag{6}$$

The gravitational force vector acting on the quad-jet and expressed in the inertial frame is given as $\{0\ 0\ mg\}^T$. This force vector is multiplied with the inverse of the Euler rotation matrix:

$$\begin{Bmatrix} F_{g_x} \\ F_{g_y} \\ F_{g_z} \end{Bmatrix} = R^T \begin{Bmatrix} 0 \\ 0 \\ mg \end{Bmatrix}, \tag{7}$$

where R^T is the inverse of Euler rotation matrix from inertial frame to body-fixed frame and m is the mass of the quad-jet. The total force acting on the quad-jet, expressed in the body-fixed frame, is

$$\mathbf{F} = \sum_{i=1}^{4} \begin{Bmatrix} F_{m_x} \\ F_{m_y} \\ F_{m_z} \end{Bmatrix}_i + \begin{Bmatrix} F_{g_x} \\ F_{g_y} \\ F_{g_z} \end{Bmatrix}. \tag{8}$$

There are three main sources of moments acting on the vehicle. These are the moments due to thrusts of jet engines (M_m), gyroscopic moments originating from jet engines (M_j), and moments caused by the drag (M_d). We can ignore the moments caused by the previously ignored drag forces. Additionally, since the mass and inertia of the aircraft are higher than the jet engine rotors, the gyroscopic moments

Table 3. Motor position vectors.

Motor no.	Position vector
1	$\mathbf{r}_1 = \{L, 0, 0\}^T$
2	$\mathbf{r}_2 = \{0, -L, 0\}^T$
3	$\mathbf{r}_3 = \{-L, 0, 0\}^T$
4	$\mathbf{r}_4 = \{0, L, 0\}^T$

acting on the aircraft due to jet engine rotor movements can be ignored in this model. The total moment acting on the vehicle will be

$$\begin{Bmatrix} M_{B_x} \\ M_{B_y} \\ M_{B_z} \end{Bmatrix} = \begin{Bmatrix} M_{m_x} \\ M_{m_y} \\ M_{m_z} \end{Bmatrix}. \tag{9}$$

To calculate the moments due to thrusts of jet engines (M_m), each motor's location on the vehicle is required. If L is the distance between each jet engine frame and vehicle body frame, then Table 3 illustrates the motor positions as given in Fig. 9.

Moments due to thrusts of jet engines (M_m) are

$$\begin{Bmatrix} M_{m_x} \\ M_{m_y} \\ M_{m_z} \end{Bmatrix}_i = \mathbf{r}_i \times \begin{Bmatrix} F_{m_x} \\ F_{m_y} \\ F_{m_z} \end{Bmatrix}_i, \tag{10}$$

$$\begin{aligned} &\{\, M_{m_x} \quad M_{m_y} \quad M_{m_z} \,\}_1^T \\ &\quad = \{\, 0 \quad -F_1 L \cos \varnothing_1 \cos \theta_1 \quad -F_1 L \sin \varnothing_1 \,\}^T, \\ &\{\, M_{m_x} \quad M_{m_y} \quad M_{m_z} \,\}_2^T \\ &\quad = \{\, -F_2 L \cos \varnothing_2 \cos \theta_2 \quad 0 \quad F_2 L \cos \varnothing_2 \sin \theta_2 \,\}^T, \\ &\{\, M_{m_x} \quad M_{m_y} \quad M_{m_z} \,\}_3^T \\ &\quad = \{\, 0 \quad F_3 L \cos \varnothing_3 \cos \theta_3 \quad F_3 L \sin \varnothing_3 \,\}^T, \\ &\{\, M_{m_x} \quad M_{m_y} \quad M_{m_z} \,\}_4^T \\ &\quad = \{\, -F_4 L \cos \varnothing_4 \cos \theta_4 \quad 0 \quad F_4 L \cos \varnothing_4 \sin \theta_4 \,\}^T. \end{aligned} \tag{11}$$

The total moment acting on the vehicle body is

$$\begin{Bmatrix} M_{m_x} \\ M_{m_y} \\ M_{m_z} \end{Bmatrix} = \sum_{i=1}^{4} \begin{Bmatrix} M_{m_x} \\ M_{m_y} \\ M_{m_z} \end{Bmatrix}_i. \tag{12}$$

3.3.1. *Engine thrust model*

In Sec. 2.1 a test stand for thrust and other data collection was presented. Once we have reliable engine data from an experiment, we implemented a thrust block in MATLAB to provide necessary thrust information to the simulation.

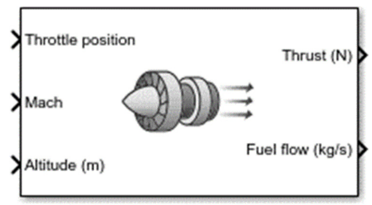

Fig. 11. The Aerospace Block set of MATLAB.

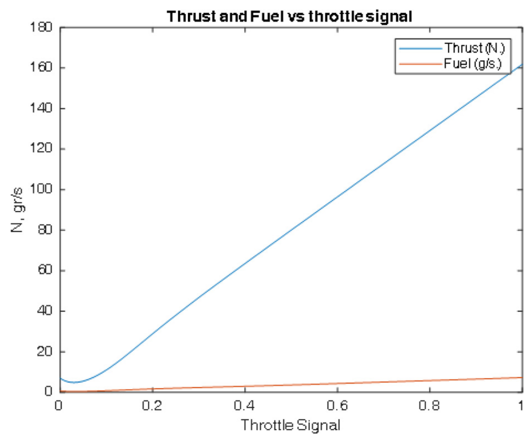

Fig. 12. The thrust force and the fuel consumption with respect to throttle percentage are calculated from the MATLAB Aerospace Block set.

The Turbofan Engine block on the Aerospace Block set of MATLAB [43] was updated with the experimental data (Fig. 11). It is a first-order representation of a turbofan engine with an engine controller. It allows thrust and weight of the fuel flow of a turbofan engine at different throttle positions (0–1). Mach number and the altitude are also considered in the block.

The thrust (N) and fuel consumption were obtained as in Fig. 12. The block permits the change of the time constant of the engine, which will be used in Sec. 4 to investigate the effect of the time constant on the vehicle control system.

4. Control System

Unlike regular four-rotor UAV systems (quadrotor or quadcopter), the control of the vehicle requires the control of four jet engine thrusts, as well as two angles for each engine, totaling 12 inputs. In this section, we propose three different controls. The first controller treats the vehicle as a quadrotor and aims to utilize thrust variations, without thrust forwarding. We aim to show that due to the motor lag, this approach will fail to stabilize the vehicle. The second approach uses a combination of thrust variation and thrust vectoring. The third control approach only uses thrust vectoring while keeping the thrust of the engines

January 5, 2022 1:20:07pm WSPC/284-US 2250001 ISSN: 2301-3850 2nd Reading

Table 4. Some properties of the quad-jet UAV.

Parameter	Value	Unit
Mass	55	kg
Inertia matrix	$\begin{bmatrix} 9 & 0 & 0 \\ 0 & 9 & 0 \\ 0 & 0 & 17 \end{bmatrix}$	kg·m^2
Center of mass–engine distance (r)	0.6	m

Table 5. States of the quad-jet UAV.

Symbol	Definition
x	Inertial frame x-position
y	Inertial frame y-position
z	Inertial frame z-position
u	Body frame x-velocity
v	Body frame y-velocity
w	Body frame z-velocity
ϕ	Euler roll angle
θ	Euler pitch angle
ψ	Euler yaw angle
p	Body frame roll rate
q	Body frame pitch rate
r	Body frame yaw rate
x_i	Inertial frame x-position integral
y_i	Inertial frame y-position integral
z_i	Inertial frame z-position integral
ϕ_ι	Euler roll angle integral
θ_ι	Euler pitch angle integral
ψ_ι	Euler yaw angle integral

constant. All of the control approaches are implemented on MATLAB Simulink.

Parameters of the quad-jet used during this analysis are shown in Table 4.

Total force vector, the moment vector, and the parameters of the quad-jet are used to solve six-degree-of-freedom equations of motion, for calculating the states given in Table 5.

We developed CAD drawings of the UAV body, jet engines, and tilting mechanisms. These CAD models were included in MATLAB simulation using Simscape (Fig. 13). This provides a visual representation of the motion of the UAV and clearly shows the motion of the jet engines.

4.1. *Control of quad-jet as a multi-rotor vehicle (without thrust vectoring)*

In this subsection, we investigated the possibility, usefulness, and limitations of the configuration in which the jet engines are installed directly to the frame without any ability to tilt them. The control is due to the varying thrust of jet motors.

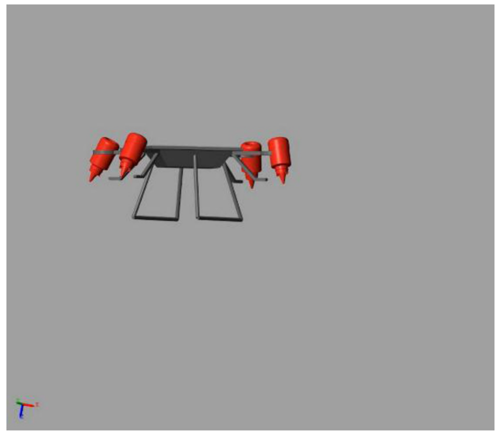

Fig. 13. The MATLAB visualization of the quad-jet motions.

This model is similar to the standard quadrotor model, in which thrust variations play a critical role in the control of the vehicle. With the engine model discussed in Sec. 3.3.1, it is possible to investigate the effects of motor time constant on the control performance.

A model, similar to the one described in Sec. 3.1, is introduced in MATLAB Simulink. Additional PID controllers for altitude, yaw, roll, and pitch are introduced. In this system, it is only possible (as in regular quadrotors) to tilt to move along x- and y-axes, we proposed two additional PID controllers to perform translational motions (Fig. 14). This model will be run with two different motor constants; 0.1 s and 1 s, to clarify the effect of motor time constant.

The first simulation was performed when the time constant is 0.1 s. The UAV goal location was set as (10,15,−5,0,0,0.4). The plot showing the UAV's translations as well as orientations is given in Fig. 15. The UAV can stabilize near the goal position with the proposed controllers. It is important to note that since jet engines are unable to produce turning moments like rotors, the vehicle cannot control yaw motion.

It is clear from Fig. 16 that there is too much chattering on throttle signals, which are limited in the range (0,1).

To investigate the effect of engine time constant, the simulation is run with time constant set to 1 s, towards the

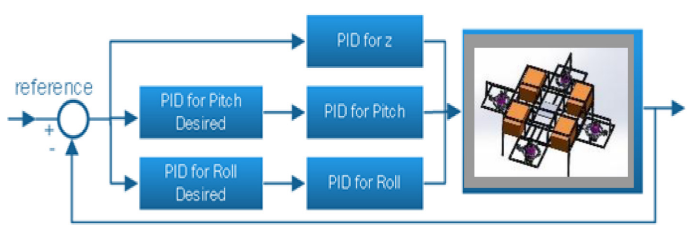

Fig. 14. PID-based controller for quad-jet that is based on thrust variations.

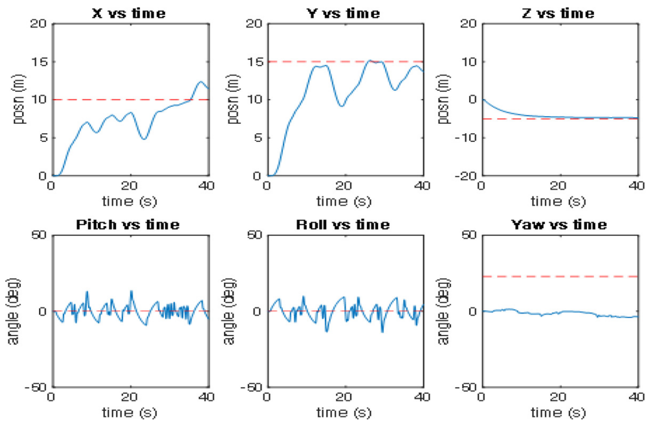

Fig. 15. Position and orientation of the quad-jet during the simulation with time constant of 0.1 s.

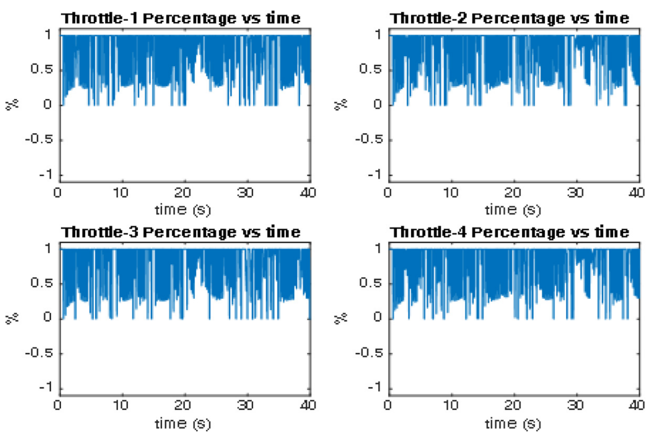

Fig. 16. Throttle percentage of the quad-jet during the simulation with time constant of 0.1 s.

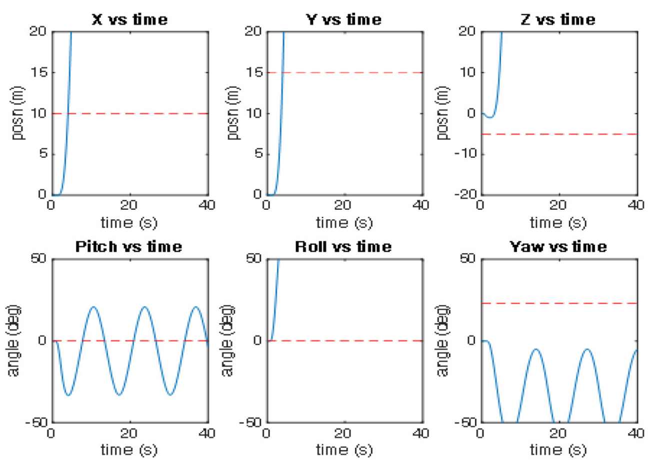

Fig. 17. Position and orientation of the quad-jet during the simulation with time constant of 1 s.

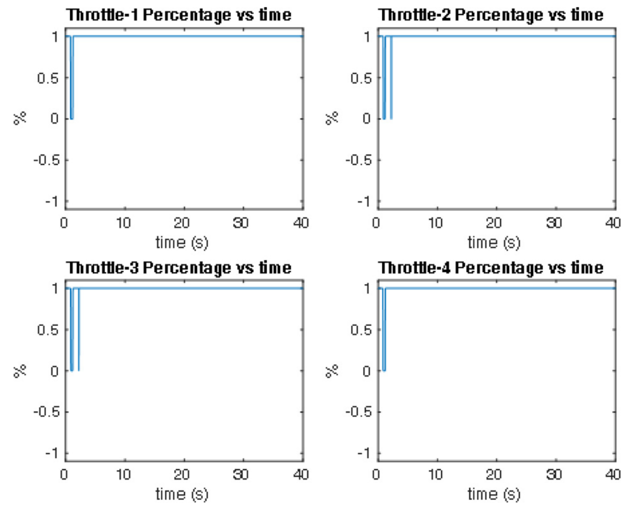

Fig. 18. Throttle percentage of the quad-jet during the simulation with time constant of 1 s.

same goal location. Simulation results shown in Fig. 17 as well as the control signals plot in Fig. 18 indicate that the vehicle is unable to provide enough control effort to stabilize the vehicle due to the lag on engines, as expected.

This analysis points out the need to use thrust vectoring mechanisms to overcome the low response time of engines to thrust variations.

4.2. *A hybrid method using thrust vectoring and thrust variations*

In this subsection, we propose a control method that uses both thrust variations as well as thrust vectoring to overcome the control problem (Fig. 19). A PID controller that can vary thrusts is used to control the altitude of the vehicle. Similarly, the roll and pitch angles are stabilized using a PID-based stabilizer using thrust variation, similar to Sec. 4.1. On the other hand, motion along x and y is controlled by tilting the jet engines with the thrust vectoring mechanisms.

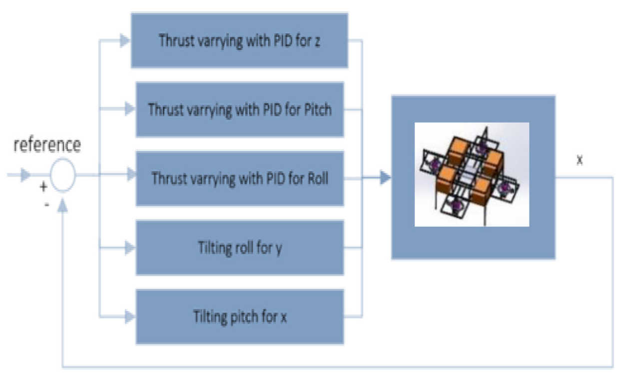

Fig. 19. Hybrid control method for controlling the quad-jet system.

January 5, 2022 1:20:28pm WSPC/284-US 2250001 ISSN: 2301-3850 2nd Reading

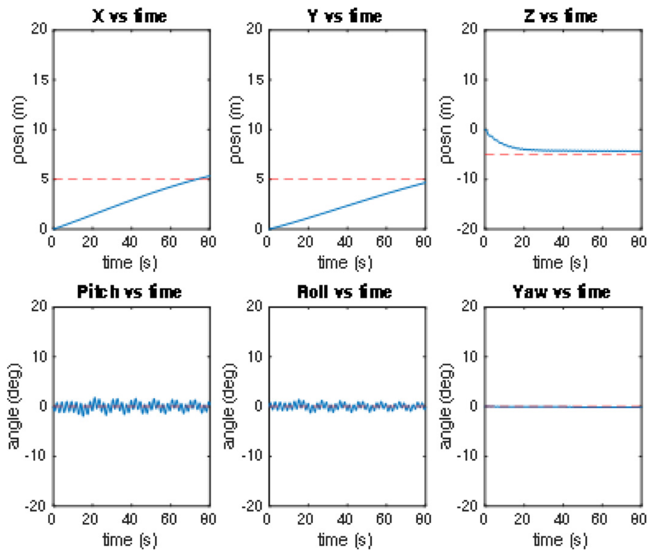

Fig. 20. Position and orientation of the quad-jet during the simulation using the hybrid control method.

In the simulation, the vehicle starts at the origin and the goal position is at (5,5,−5,0,0,0). The position and orientation of the vehicle (Fig. 20) during the simulation show that the controller can stabilize and move the vehicle to the goal position, successfully.

Although control signals (Fig. 21) show chattering (due to high-frequency roll and pitch angles of the tilting mechanism to move the vehicle to the goal location), the vehicle can be stabilized using this controller, even though motor time constant is 1 s.

This analysis points out the combined benefit of thrust variations and tilting the engines. We should point out that this approach has the additional benefit of the ability to move along x or y-axis without tilting the vehicle body. This could be quite advantageous on operations such as aerial filming and surveillance.

4.3. *Control of quad-jet with the thrust vectoring only*

The quad-jet system requires 12 inputs. Eight inputs are the angles of the thrust vectoring mechanisms, and the others are the jet engine thrust inputs. Now, let us propose another controller that uses only those angles of thrust vectoring while keeping the thrust values constant during operation (Fig. 22). This approach will enable the vehicle to overcome the slow characteristics of jet engines.

One possible control approach can be the full-state feedback control [44]. In this approach, a control signal $u = -Kx$, where K is a matrix, is used to stabilize the system. One can use the pole placement approach and put poles in the desired location on the left half-plane, and therefore identify the desired characteristic equation and identify a suitable K matrix. In this system, we have a state of 12 elements and a nonlinear plant. To implement full-state feedback let us first linearize the plant, and then apply Linear Quadratic Regulator to find an unknown K matrix. This linearization is only performed to develop the controller. The vehicle model is still nonlinear.

To implement a linear controller, the first step is to linearize the quad-jet model, already developed in MATLAB. The states of the model are: $x = (x\ y\ z\ u\ v\ w\ \phi\ \theta\ \psi\ p\ q\ r\ x_i\ y_i\ z_i\ \phi_i\ \theta_i\ \psi_i)^T$, and the inputs are chosen as: $u = (\phi_1\ \theta_1\ \phi_2\ \theta_2\ \phi_3\ \theta_3\ \phi_4\ \theta_4)^T$. Here, we assume that all of the states are measurable.

The system is numerically linearized around a specific trim condition, where all states are controllable, and the jet quadrotor hovers. This has been done in MATLAB with *linmod* function. This approach provided a linear

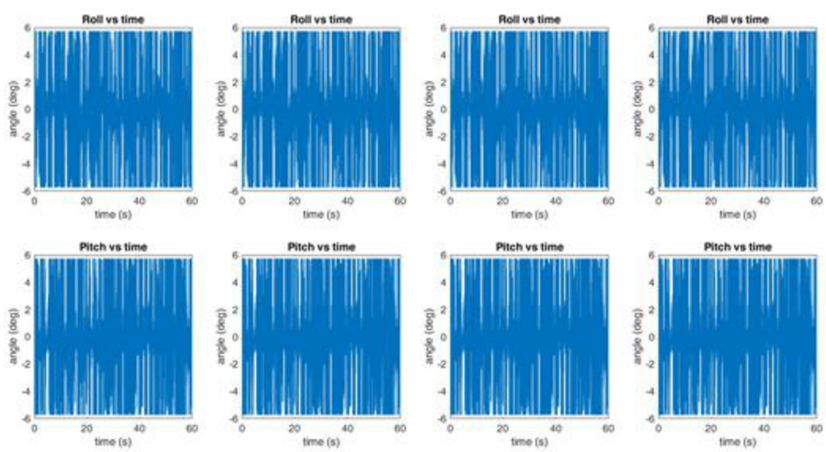

Fig. 21. The roll and pitch values of the thrust vectoring mechanisms (during hybrid control column 1 is for first motor, column 2 is for second motor, and vice versa).

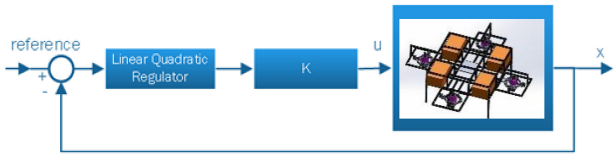

Fig. 22. Control approach based on full-state feedback using LQR for control of the quad-jet, without thrust variations.

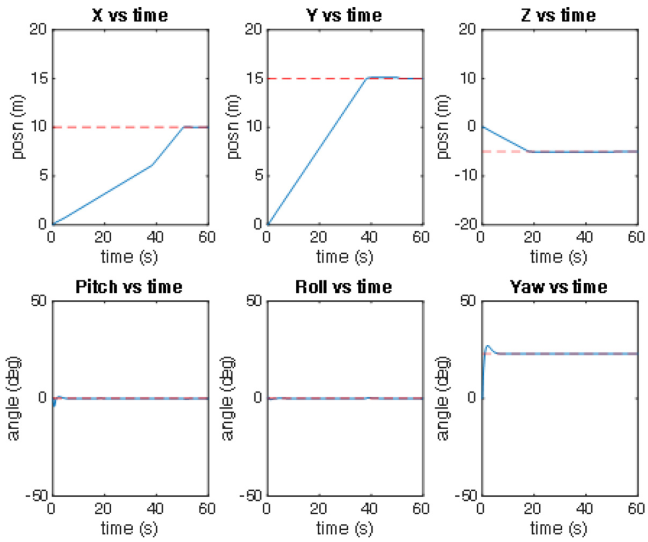

Fig. 23. Position and orientation of the quad-jet during the simulation using the LQR controller.

state-space model given of the quad-jet as

$$\begin{aligned} \dot{x} &= A_{18\times 18}x + B_{18\times 8}u \\ y &= C_{18\times 18}x + D_{18\times 8}u \end{aligned} \tag{13}$$

To implement a full-state feedback controller, one needs to check controllability. All of the states of the linearized system are found to be fully controllable. Once the linear model is ready, one can implement the LQR method to determine the K matrix to be used in the input, $u = -Kx$.

Additionally, to eliminate steady-state error, integral action has been added to the state, leading to a state of size 18 elements. The required K was calculated using the MATLAB

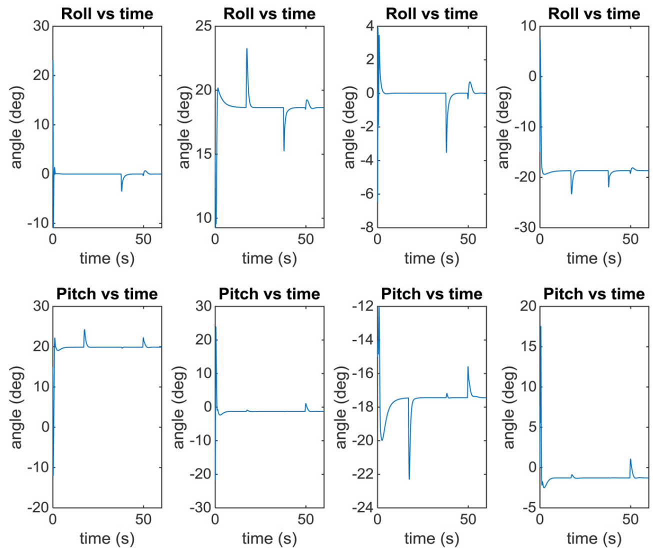

Fig. 24. The roll and pitch values of the thrust vectoring mechanisms (during LQR control column 1 is for first motor, column 2 is for second motor, and vice versa).

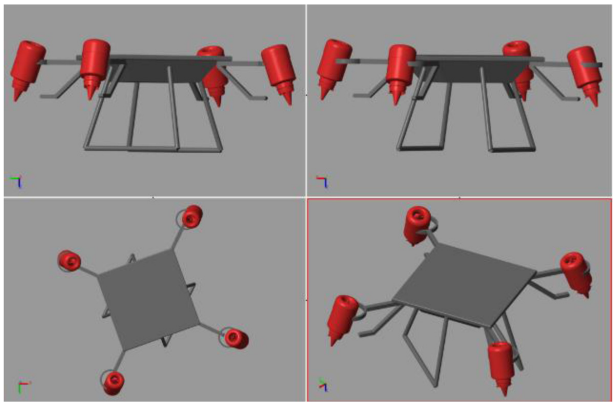

Fig. 25. The vehicle during the simulation.

lqr function, using the matrices $Q = I_{18\times 18}$ and $R = I_{8\times 8}$ and the system is given in Sec. 3. Having a suitable K matrix is not enough for stability. We investigated the closed-loop stability of the system by verifying that all closed-loop system poles stay on the left half of the complex plane, leading to a stable response.

Table 6. Comparison of proposed controllers.

Controller 1	Controller 2	Controller 3
Sensitive to the motor time constant	Not sensitive to the motor time constant	Not sensitive to the motor time constant
Cannot control vehicle yaw	Can control vehicle yaw	Can control vehicle yaw
Too much chattering	Too much chattering	No chattering
The vehicle body has to be tilted for motion	The vehicle body can be flat during motion	The vehicle body can be flat during motion

In order to investigate the control performance, the simulation run with time constant set to 1 s, towards the goal location (10, 15,−5,0,0,0.4).

The position and orientation of the quad-jet in Fig. 23 verifies that the vehicle could easily reach the goal position. The roll and pitch angles of each jet engine are presented in Fig. 24. The vehicle hovering at the final location is shown in Fig. 25.

Proposed controllers are compared in Table 6. Considering the controllers proposed in this work, it is clear that the last controller performs better in controlling the quad-jet aircraft. The vehicle could reach the goal position successfully. The control effort is directed more intelligently and it is better than the controllers 1 and 2. Besides, yaw control is possible in controller 3. It is important to note that since the engine settles down at a constant speed of rotation only once at the beginning, the time constant of the engines does not play an important effect on system performance. Moreover, the vehicle body does not tilt or roll towards the goal location, unlike regular quadrotor vehicles. The thrust vectoring system directs jet engines as required so that the aircraft body stays flat. This leads to a more stable flight that is desirable in aerial filming, parcel delivery, and autonomous taxi operations.

5. Conclusions and Future Work

In this paper, we proposed a mini jet engine-powered UAV (called quad-jet). Unlike electric motors, jet engine thrust cannot be varied rapidly. To overcome this problem, we designed a mechanism to tilt and roll each jet engine (thrust vectoring). The increased thrust due to jet engines promises increased payload capacity, flight time, or flight range.

We introduced the design, modeling, and control of this vehicle. Three different controllers were suggested and all were tested in simulations in MATLAB Simulink. A PID-based controller depending on thrust variations failed when the engine response time is big. A hybrid controller including the PID-based altitude and attitude controllers (based on thrust variation) and additional controllers that relate engine tilting to x- and y-axes motions of the vehicle were also suggested and tested. In the analysis, the motor time constant was used as 1 s, but many mini jet engines have a time constant of 2 s or 3 s, which worsens the control performance. It was shown that a full-state feedback controller using an LQR control strategy to control tilt angles of engines is a better control action than the proposed alternatives to stabilize the vehicle, and it is not sensitive to the motor time constant.

The ability of vector thrusting proved to be suitable to overcome the effects of engine response delay on jet-powered systems and can be used on jet-engined UAV systems.

Our future work will include manufacturing, flight tests of a prototype to verify thrust forwarding and suitability of the proposed system to autonomous operation in various real-world, civilian applications.

Acknowledgments

This project has been funded by the Scientific and Technological Research Council of Turkey (TÜBİTAK) with the Project No. 118E192.

References

[1] P. Castillo, R. Lozano and A. E. Dzul, *Modeling and Control of Mini-Flying Machines*, Advances in Industrial Control (Springer, 2005).
[2] D. Suter, T. Hamel and R. Mahony, Visual servo control using homography estimation for the stabilization of an X4 flyer, in *Proc. 41st IEEE Conf. Decision and Control* (2002), pp. 2872–2877.
[3] T. Hamel, R. Mahony, R. Lozano and J. Ostrowski, Dynamic modeling and configuration stabilization for an X4-flyer, *IFAC Proc. Vol.* **35** (2002) 217–222.
[4] A. Tayebi and S. McGilvray, Attitude stabilization of a VTOL quadrotor aircraft, *IEEE Trans. Control Syst. Technol.* **14**(3) (2006) 562–571.
[5] J. Escareno, S. Salazar-Cruz and R. Lozano, Embedded control of a four-rotor UAV, in *Proc. American Control Conf.* (2006), pp. 189–204.
[6] P. Castillo, A. E. Dzul and R. Lozano, Real-time stabilization and tracking of a four-rotor mini rotorcraft, *IEEE Trans. Control Syst. Technol.* **12**(4) (2004) 510–516.
[7] E. Altuğ, J. P. Ostrowski and C. J. Taylor, Control of a quadrotor helicopter using dual camera visual feedback, *Int. J. Robot. Res.* **24**(5) (2005) 329–341.
[8] S. Bouabdallah and R. Siegwart, Backstepping and sliding-mode techniques applied to an indoor micro quadrotor, *Proc. 2005 IEEE Conf. Robotics and Automation* (2005), pp. 2247–2252.
[9] C. Soares, *Gas Turbines: A Handbook of Air, Land and Sea Applications* (Butterworth-Heinemann, 2014).
[10] M. Rogers, *VTOL Military Research Aircraft* (Haynes Publishing Group, 1989).
[11] http://www.jetcat.de/de/.
[12] http://www.kingtechturbines.com/products/.
[13] http://www.hyblturbines.cz/.
[14] http://www.atj.com.tw/.
[15] http://www.jetcentralusa.com/.
[16] C. Polat, An electronic control unit design for a miniature jet engine (Küçük bir jet motoru icin elektronik kontrol ünitesi tasarımı), Master's thesis, Middle East Technical University (2009).
[17] Ö. Mutlu, Küçük ölçekli turbo jet motor modellemesi ve kontrolü, Master's thesis, Istanbul Technical University (2015).
[18] https://zapata.com/air-products/flyboardair.
[19] Y. Long and D. J. Cappalleri, Linear control design, allocation, and implementation for the omnicopter MAV, in *Proc. 2013 IEEE Int. Conf. Robotics and Automation* (2013), pp. 289–294.
[20] M. Muehlebach and R. D'Andrea, The Flying Platform — A testbed for ducted fan actuation and control design, *Mechatronics* **42** (2017) 52–68.
[21] D. Wiegand, Vertical take-off aircraft, US Patent Application No. US20160023754A1 (2014).
[22] https://lilium.com/technology/.

[23] H. Yeo and W. Johnson, Performance and design investigation of heavy lift tilt-rotor with aerodynamic interference effects, *J. Aircr.* **46**(4) (2009) 1231–1239.
[24] H. V. Borst, Design and development considerations of the X-19 VTOL aircraft, *Ann. N. Y. Acad. Sci.* **107** (1963) 265–279.
[25] M. J. Hirschberg, An overview of the history of vertical and/or short take-off and landing (V/STOL) aircraft (2006), http://www.vstol.org.
[26] M. Sklar, Diversity in design, Integrated Defense Systems, *Boeing Frontiers*, December 2006/January 2007 (2006), pp. 44–45.
[27] E. Çetinsoy, S. Dikyar, C. Hancer, K. T. Oner, E. Sirimoglu, M. Unel and M. F. Aksit, Design and construction of a novel quad tilt-wing UAV, *Mechatronics* **22** (2012) 723–745.
[28] M. Ryll, H. H. Bülthoff and P. R. Giordano, Modeling and control of a quadrotor UAV with tilting propellers, in *Proc. 2012 IEEE Int. Conf. Robotics and Automation* (2012), pp. 4606–4613.
[29] S. H. Jeong and S. Jung, Novel design and position control of an omnidirectional flying automobile (Omni-Flymobile), in *Proc. Int. Conf. Control, Automation and Systems* (2010), pp. 2480–2484.
[30] S. Salazar-Cruz, R. Lozano and J. Escaren, Stabilization and nonlinear control for a novel trirotor mini-aircraft, *Control Eng. Pract.* **17** (2009) 886–894.
[31] http://www.aviastar.org/helicopters_eng/bell_qtr.php.
[32] F. Şenkul and E. Altuğ, Modeling and control of a novel tilt–roll rotor quadrotor UAV, in *Proc. 2013 IEEE Int. Conf. Unmanned Aircraft Systems* (2013), pp. 1071–1076.
[33] F. Şenkul and E. Altuğ, Adaptive control of a tilt–roll rotor quadrotor UAV, in *Proc. 2014 IEEE Int. Conf. Unmanned Aircraft Systems* (2014), pp. 1132–1137.
[34] F. Şenkul and E. Altuğ, System design of a novel tilt-roll rotor quadrotor UAV, *J. Intell. Robot. Syst.* **84** (2016) 575–599.
[35] F. Şenkul, Ş. Y. Gelbal and E. Altuğ, Manufacturing and flight tests of a quadrotor UAS with tiltable rotors, in *Proc. 2016 Int. Conf. Unmanned Aircraft Systems* (2016).
[36] http://edition.cnn.com/2017/03/17/tech/ehang-passenger-drone-dubai/index.html.
[37] H. Voos, Nonlinear control of a quadrotor micro-UAV using feedback-linearization, in *Proc. 2009 IEEE Int. Conf. Mechatronics* (2009), pp. 3–6.
[38] F. Sabatino, Quadrotor control: Modeling, nonlinear control design, and simulation, Master's thesis, KTH Royal Institute of Technology (2015).
[39] M. Hofer, M. Muehlebach and R. D'Andrea, Application of an approximate model predictive control scheme on an unmanned aerial vehicle, in *Proc. 2016 IEEE Int. Conf. Robotics and Automation* (2016), pp. 2952–2957.
[40] C. Sferrazza, M. Muehlebach and R. D'Andrea, Trajectory tracking and iterative learning on an unmanned aerial vehicle using parametrized model predictive control, in *Proc. 2017 IEEE 56th Annu. Conf. Decision and Control* (2017), pp. 5186–5192.
[41] M. Muehlebach and R. D'Andrea, The Flying Platform — A testbed for ducted fan actuation and control design, *Mechatronics* **42** (2017) 52–68.
[42] M. Neunert, C. De Crousaz, F. Furrer, M. Kamel, F. Farshidian, R. Siegwart and J. Buchli, Fast nonlinear model predictive control for unified trajectory optimization and tracking, in *Proc. 2016 IEEE Int. Conf. Robotics and Automation* (2016), pp. 1398–1404.
[43] M. Murray, *Optimization-Based Control* (California Institute of Technology, 2009).
[44] The MathWorks, Inc., MATLAB (2010), version 7.10.0 (R2010a).
[45] K. Ogata, *Modern Control Engineering* (Prentice Hall, 2010).

Erdinç Altuğ received his M.S. degree in Mechanical Engineering from the Carnegie Mellon University, USA, and his Ph.D. degree in Engineering and Applied Mechanics from the University of Pennsylvania, USA, in 1999 and 2003, respectively. Since 2004, he has been working at the Istanbul Technical University, Turkey. He is currently an Associate Professor in the Department of Mechanical Engineering, Istanbul Technical University. Since 2015, he serves as a Director of the Autonomous Systems Research Laboratory, where he is responsible for research projects in the area of autonomous systems.

Erdinç is the author of over 58 technical publications. His research interests include the design and control of unmanned aerial and ground vehicles.

Abdullah Türkmen received his B.S. and M.S. degrees from the Istanbul Technical University, Turkey, in 2017 and 2019, respectively. From 2017 to 2020, he was a Researcher at the Autonomous Systems Research Laboratory, and worked on the quad-jet project.

His research interests include the design and control of mechatronic systems.